Spectral windows analysis method for monitoring anthropogenic radionuclides in real-time environmental gamma-ray scintillation spectrometry

To cite this article before publication: Elena Prieto *et al* 2017 *J. Radiol. Prot.* in press https://doi.org/10.1088/1361-6498/aa9b9c

Spectral windows analysis method for monitoring anthropogenic radionuclides in real-time environmental gamma-ray scintillation spectrometry

E. Prieto[1], R. Casanovas[1] and M. Salvadó[1].

[1] Unitat de Física Mèdica, Facultat de Medicina i Ciències de la Salut, Universitat Rovira i Virgili, Sant Llorenç 21, ES-43201 Reus (Tarragona), Spain.

Abstract

This paper proposes an analysis methodology based on the spectral windows technique aimed for environmental real-time gamma-ray spectra obtained with scintillation detectors. The method permits to monitor activity concentrations of selected isotopes, such as anthropogenic radionuclides like ^{137}Cs and ^{131}I, by removing the Compton scattering plus other external contributions and resolving peak overlapping within any window. Activity concentrations are presented for ^{137}Cs, ^{131}I, ^{214}Bi and ^{214}Pb when applying the method to a monitor using a $LaBr_3$(Ce) detector. The method avoids false-positive and false-negative results of anthropogenic radionuclides in presence of radiation from natural origin obtaining activity concentrations that correspond to those obtained by a Gaussian fitting commercial software.

Key words: **scintillation gamma-ray spectrometry, real-time, $LaBr_3$(Ce), ^{137}Cs, ^{131}I, windows technique, activity concentration**

1 Introduction

Over the past few years, the Medical Physics Unit of *Universitat Rovira i Virgili* has participated in a project for the improvement of the automatic real-time environmental surveillance network of Catalonia (ES-E, Spain-East) [1]. The main development of the project has been the implementation of gamma-ray scintillation spectrometry monitors with NaI(Tl) and $LaBr_3$(Ce) scintillation detectors all over the region and, specially, around the two nuclear power plants that operate in the area.

The monitors implemented in the Catalan network were developed for aerosol surveillance using a particulate filter (RARM-F) [2] and for measuring directly to the environment using two shielded detectors (RARM-D2) [3], with either NaI(Tl) or $LaBr_3$(Ce) detectors. Additionally, two water NaI(Tl) monitors [4] were developed and also tested using a $LaBr_3$(Ce) detector [5] for the surveillance of the water from Ebre river, which is used for cooling the two pressurised water reactors of one of the nuclear power plants.

Recently, a variety of direct monitors without shielding have been incorporated to the network, comprising different scintillation materials and crystals sizes: 1”×1” and 2”×2” $LaBr_3$(Ce) detectors and 2”×2” and 3”×3” NaI(Tl) detectors. At present, there are a total of 26 installed monitors in the network using scintillation gamma-ray spectrometry that are measuring in real-time, providing new spectra every 10 minutes. Thus, the total quantity of data to be analysed every day is very large.

Spectra registered in short integration times usually present high noise and low statistics due to environmental low dose rate measures, and hence, conventional peak analysis of gamma-ray spectra may not be accurate in providing real-time results. For this, other analysis methods that permit to establish early-warning alarms need to be developed to maximize the information extracted from these spectra, such as obtaining the ambient dose equivalent H*(10) from gamma-ray spectra [6] or using spectral windows analysis methods [7][8][9][10][11][12].

In this study, a novel spectral windows method was developed to automatically monitor anthropogenic isotopes activity concentrations. The developed algorithm compensates the natural radioactivity oscillations, especially those associated with ^{222}Rn daughters (RD) that are related to meteorological variations (mainly rain and humidity variations). Besides, the algorithm not

only considers the overlapping of the target anthropogenic isotopes peaks with the natural radiation ones but also accounts for the surplus of counts generated as a consequence of Compton dispersion arising from natural radiation that affects the entire spectrum.

The developed algorithm was optimized and tested for measuring ^{131}I and ^{137}Cs activity concentrations in real-time with a 2"×2" $LaBr_3$(Ce) detector measuring directly to the environment in different backgrounds.

2 Materials

2.1 Equipment and data acquisition

The detector used in this study was a 2"×2" $LaBr_3$(Ce) BrilLance^{TM}380 from Saint-Gobain Crystals® that was coupled to a digital multichannel analyser (Digibase from ORTEC®). Experimental data were obtained using radioactive sources: a point-like source of ^{137}Cs, a hermetically sealed source of ^{226}Ra in equilibrium with its gamma emitter daughters of ^{222}Rn (mainly ^{214}Pb and ^{214}Bi) and an encapsulated source of ^{131}I.

The detector and the radioactive sources were placed at 1.5 m above the ground, coupled to a stick, to guarantee an isotropic radiation field by avoiding its interference with the laboratory objects, walls and floor. All acquired spectra were collected during a 10 min integration time at different detector-source distances to simulate different airborne activity concentrations. The Gaussian peak analysis of spectra was performed using the commercial software ScintiVision^{TM} from ORTEC®, whereas the operations related with spectral windows were carried out by means of an internally developed software.

3 Methods

3.1 Spectra stabilisation and detector calibrations

Before the application of any analysis method, registered spectra need to be stabilised and calibrated in energy. Besides, to perform activity concentration calculations, resolution and efficiency calibrations are also necessary.

3.1.1 Spectra stabilisation

Spectra stabilisation is required to correct the peak shift that is observed in spectra, basically due to ambient temperature variations. A self-developed software was used to apply a previously described methodology that automatically searches for reference peaks, compares their current position with a reference positionand corrects the entire spectrum [13].

3.1.2 Energy and resolution calibrations

The energy and resolution calibrations were performed using the radioactive sources listed in Section 2.1. The optimal fitting functions for these calibrations were set in a previous study [14]. Thus, the energy calibration was set using the following equation:

$$E = a_0 + a_1 \cdot C + a_2 \cdot C^2 \quad (1)$$

where C is the channel number, E is the energy and a_k are the fitting coefficients.

For the resolution calibration, the following 2nd-order polynomial was used to fit the experimental data:

$$FWHM(E) = b_0 + b_1 \cdot E + b_2 \cdot E^2 \quad (2)$$

where *FWHM(E)* is the Full Width at Half Maximum, E is the energy and b_k are the fitting coefficients.

3.1.3 Efficiency calibration

Finally, to obtain activity concentrations, an efficiency calibration was performed using Monte Carlo simulations with EGS5 code. The isotopes were assumed to be homogeneously distributed in air, forming a cylindrical source of equal radius and diameter of 500 m ("infinite" source) surrounding the $LaBr_3$(Ce) detector. More details about this calibration together with the obtained results were given in a previous study [3].

The assumption of this isotope distribution is necessary to quantify activity concentrations; however, it could not represent the real geometry of the source. In the event of a real emission of anthropogenic radionuclides requiring a depth study, the efficiency could be recalculated to account the particularities of the radioactive plume, and thus, obtaining more accurate values for activity concentrations.

It should be noted that the radioactive sources used in this study (see section 2.1) do not correspond to the assumed geometry, but taking into account the purposes of this paper, they were considered as if.

3.2 Description of the method

3.2.1 ROI width determination

The width of the spectral windows or ROIs (Region of Interest) was determined by the width of the expected peaks of the isotopes of study, which is proportional to the Full Width at Half Maximum (FWHM) in function of the energy that is obtained in the resolution calibration:

$$n = n(E) = k \cdot FWHM(E) \quad (3)$$

where k is the proportionality constant to set the desired peak coverage and *FWHM(E)* is a 2nd degree polynomial function of the energy (E). In this study, the widths of all the ROIs used where set at $k = 1.699$ for a 95.45% peak area coverage.

Given that the chosen width of the ROIs does not cover the entire Gaussian distribution arising from a gamma emission in a spectrum taken with scintillation detectors, the activity of the studied isotope in a ROI is calculated as:

$$A = \frac{cps}{\varepsilon \cdot p_\gamma \cdot G} \quad (4)$$

where cps is the number of counts per second in the given ROI, ε is the detector efficiency, p_γ is the emission probability of the gamma-ray and G is a term that corrects the proportion of Gaussian distribution that covers the width of the ROI, as it does not include the entire Gaussian

distribution and hence, not all the cps originated from the gamma emission would be counted in the activity calculation.

3.2.2 **Compton scattering and other contributions to spectra**

When a gamma-ray spectrum is obtained with scintillation detectors, only a portion of the total cps is significant to calculate activity concentrations. These cps are those under the photo-peak and above the baseline of the Gaussian distribution. The rest of cps of the spectrum is a result from different interactions between gamma-rays or beta particles and the detector materials, such as the Compton scattering.

In an environmental gamma-ray spectrum, the amount of cps arising from Compton scattering could be divided in two groups: the Compton contribution originated from gamma-ray emitting RD (mainly ^{214}Bi and ^{214}Pb) and the Compton contribution from all the other natural radionuclides such as ^{40}K and gamma-ray emitting isotopes from ^{232}Th decay chain (mainly ^{208}Tl, ^{228}Ac, ^{212}Pb or ^{212}Bi).

Moreover, other phenomena provide extra counts to gamma-ray spectra obtained with scintillation detectors. Among these are random summing, which is the continuum above the full energy-peaks, pair production (the annihilation peak at 511 keV) or Bremsstrahlung radiation that is registered in the low energy range of a spectrum and it is due to high-energy beta particles. In addition, in spectra obtained with lead shielded detectors peaks arising from characteristic X-rays or Compton backscattering in the region of 200-300 keV are also found [15].

In this regard, the developed methodology hypothesises that the amount of Compton scattering plus all the associated external counts from other interaction phenomena due to RD, in a certain window or ROI, is considered to be proportional to ^{214}Bi activity concentration (A_{Bi}), as the latter isotope is mainly in equilibrium with ^{214}Pb. Thus, the external contribution due to RD is:

$$RD\_cont_i = m_i \cdot A_{Bi} \tag{5}$$

where RD_cont_i is the external contribution from Compton scattering plus other interaction phenomena due to RD in ROI$_i$ (in cps), m_i is the fitting coefficient and A_{Bi} is ^{214}Bi activity concentration (Bq/m^3).

On the other hand, the amount of Compton scattering from the rest of natural radionuclides plus other possible types of contributions to a spectrum is considered to be constant. Thus, from Equation (5), the total extra cps contribution to a ROI can be written as:

$$cont_i = m_i \cdot A_{Bi} + c_i \tag{6}$$

where $cont_i$ is the total extra cps contribution in ROI$_i$ and c_i is the Compton scattering plus other interaction phenomena due to non-RD natural emissions. (The total extra contribution to a ROI is shown in black in Figure 1).

3.2.3 **Peak overlapping**

Peak overlapping occurs when some cps from two Gaussian distributions arising from different gamma emissions are found inside the same ROI. The components (in cps) of two adjacent ROIs centred in two gamma emissions of different isotopes that present peak overlapping can be identified as follows:

$$ROI_1 = cps_{11} + cps_{21} + cont_1 + Bkgd_1 \quad (7)$$

$$ROI_2 = cps_{22} + cps_{12} + cont_2 + Bkgd_2 \quad (8)$$

where ROI_1 are all the cps contained in the ROI centred around the gamma emission of isotope 1, cps_{11} are the cps of isotope 1 in ROI_1, cps_{21} are the cps of isotope 2 in ROI_1, $cont_1$ is the total extra cps contribution in ROI_1 and $Bkgd_1$ are the cps of the intrinsic background in ROI_1. Analogously, ROI_2 are all the cps contained in the ROI centred around the gamma emission of isotope 2, cps_{22} are the cps of isotope 2 in ROI_2, cps_{12} are the cps of isotope 1 in ROI_2, $cont_2$ is the total extra cps contribution in ROI_2 and $Bkgd_2$ are the cps of the intrinsic background in ROI_2.

The term $Bkgd_i$ was included to take into account those detectors that have an intrinsic self-activity, such as $LaBr_3$(Ce) or $LaCl_3$(Ce) detectors (see Section 3.3). To apply the methodology at spectra obtained with detectors without self-activity, such as NaI(Tl), this term should not be considered.

Figure 1 shows the composition of two ROIs in cps, ROI_1 and ROI_2, corresponding to two close gamma emissions originated from isotope$_1$ and isotope$_2$ in a reproduction of a spectrum obtained with a $LaBr_3$(Ce) detector. The Gaussian distributions of the emissions are drawn to identify the peak overlapping: the widths of ROI_1 and ROI_2 are smaller than the full energy peaks of the gamma emissions but contain cps of both isotopes.

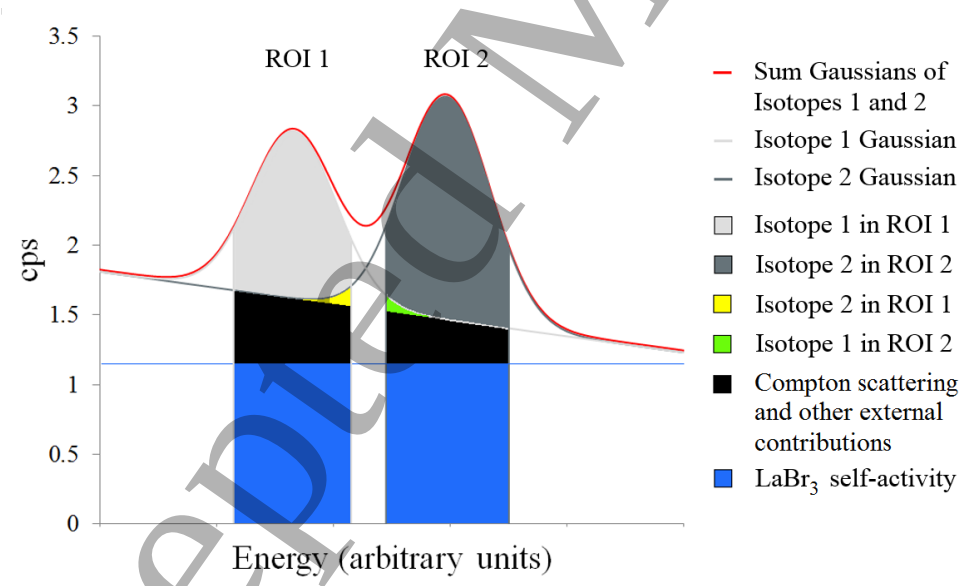

Figure 1. Composition of two ROIs in a partial reproduction of a $LaBr_3$(Ce) spectrum with two overlapped energy peaks. (For interpretation of the references to colour in this figure legend, the reader is referred to the web version of this article.)

The cps originated from a gamma emission of an isotope *i* in a given ROI *j* can be written in terms of the isotope activity concentration using Equation(4):

$$cps_{ij} = A_i \cdot p_i \cdot \varepsilon_i \cdot G_{ij} \tag{9}$$

where cps_{ij} are the cps of isotope i in ROI j, A_i is the activity concentration of isotope i, p_i is the probability of the emission of isotope i, ε_i is the detector efficiency of the emission of isotope i and G_{ij} is the term that takes into account the proportion of the Gaussian distribution of isotope i inside ROI j.

Using Equations (6) and(9), Equations (7) and (8) can be written as:

$$ROI_1 = A_1 \cdot p_1 \cdot \varepsilon_1 \cdot G_{11} + A_2 \cdot p_2 \cdot \varepsilon_2 \cdot G_{21} + m_1 \cdot A_{Bi} + c_1 + Bkgd_1 \tag{10}$$

$$ROI_2 = A_2 \cdot p_2 \cdot \varepsilon_2 \cdot G_{22} + A_1 \cdot p_1 \cdot \varepsilon_1 \cdot G_{12} + m_2 \cdot A_{Bi} + c_2 + Bkgd_2 \tag{11}$$

Solving the equation system, the activities of the isotopes, A_1 and A_2, can be obtained:

$$A_1 = \frac{ROI_1 - Bkgd_1 - m_1 \cdot A_{Bi} - c_1 - \left(ROI_2 - Bkgd_2 - m_2 \cdot A_{Bi} - c_2\right)\left(\frac{G_{21}}{G_{22}}\right)}{p_1 \cdot \varepsilon_1 \left(G_{11} - \frac{G_{12} \cdot G_{21}}{G_{22}}\right)} \tag{12}$$

$$A_2 = \frac{ROI_2 - Bkgd_2 - m_2 \cdot A_{Bi} - c_2 - \left(ROI_1 - Bkgd_1 - m_1 \cdot A_{Bi} - c_1\right)\left(\frac{G_{12}}{G_{11}}\right)}{p_2 \cdot \varepsilon_2 \left(G_{22} - \frac{G_{21} \cdot G_{12}}{G_{11}}\right)} \tag{13}$$

3.2.4 **Determination of m_i and c_i**

As mentioned before in Equation(6), the total external contribution in a ROI was considered to be the Compton scattering contribution from RD, which is assumed to be m_i-proportional to A_{Bi}, plus the Compton scattering from the rest of natural emissions and other external contributions (c_i), which is assumed to be constant.

The determination of m_i and c_i was performed for the $LaBr_3$(Ce) detector using the radioactive sources listed in Section 2.1 to ensure that the algorithm is optimised for detecting small amounts of ^{137}Cs and ^{131}I over a natural background with changing radon and RD concentrations. The obtained spectra encompass different combinations of sources placed at different distances to simulate different activity concentrations of airborne isotopes. Determination of fitting coefficients was performed using a background spectrum, a ^{226}Ra spectrum, a ^{137}Cs spectrum and a ^{226}Ra with ^{131}I spectrum (it should be noted that the spectra used for the determination of the parameters are different from those used to test the methodology in Section 4).

The activity concentrations of different isotopes (^{214}Pb, ^{131}I, ^{208}Tl, ^{214}Bi and ^{137}Cs) were determined for each spectrum using ScintiVision™ software by fitting Gaussian peaks. The activity concentration of the chosen isotopes could be alternatively obtained applying Equations (12) and(13), considering that the ROIs of these isotopes in a $LaBr_3$(Ce) detector partially overlap with others. By way of example: ^{214}Pb (352 keV) overlaps with ^{131}I (365 keV), ^{208}Tl (583 keV) overlaps with ^{214}Bi (609 keV) and ^{137}Cs (662 keV) overlaps with ^{214}Bi (665 keV).

Therefore, the values of the obtained activities by Gaussian fitting for each spectrum were substituted in Equations (12) and(13), along with the other known parameters of the equations, such as the total value of the ROIs, the intrinsic background of the ROIs, the peak covertures *G*, the emission probabilities and the efficiencies. Thus, a set of equations that covered a variety of real radioactive sources contributions was obtained, where the only unknown parameters were m_i and c_i. Using a calculation programme, a least squares fit was applied to obtain the values of m_i and c_i that adjusted to all the equations at the same time.

3.2.5 **Peak overlapping with ^{214}Bi**

The method described to obtain the activities of overlapped peaks requires a previous assessment of ^{214}Bi activity concentration. The activity concentration of ^{214}Bi can be obtained from its most probable emission (609 keV) using Equation(12), as it partially overlaps with an emission from ^{208}Tl at 583 keV. Therefore, the term A_{Bi} in Equations (12) and (13) is calculated previously as:

$$A_{Bi} = \frac{ROI_{Bi} - Bkgd_{Bi} - c_{Bi} - \left(ROI_{Tl} - Bkgd_{Tl} - c_{Tl}\right)\left(\frac{G_{TlBi}}{G_{BiBi}}\right)}{p_{Bi}\cdot\varepsilon_{Bi}\left(G_{BiBi} - \frac{G_{BiTl}\cdot G_{TlBi}}{G_{TlTl}}\right) + m_{Bi} - m_{Tl}\frac{G_{TlBi}}{G_{TlTl}}} \quad (14)$$

where ROI_{Bi} is the ROI centred around the 609 keV peak of ^{214}Bi, $Bkgd_{Bi}$ is the $LaBr_3$(Ce) intrinsic background in ROI_{Bi}, c_{Bi} is the contribution from Compton scattering plus other interaction phenomena due to non-RD natural emissions to ROI_{Bi}, ROI_{Tl} is the ROI centred around the 583 keV peak of ^{208}Tl, $Bkgd_{Tl}$ is the intrinsic background in ROI_{Tl}, c_{Tl} is the contribution from Compton scattering plus other interaction phenomena due to non-RD natural emissions to ROI_{Tl}, G_{TlBi} is the amount of ^{208}Tl Gaussian distribution inside ROI_{Bi}, G_{BiBi} is the amount of ^{214}Bi Gaussian distribution inside ROI_{Bi}, p_{Bi} is the probability of the 609 keV emission from ^{214}Bi, ε_{Bi} is the detector efficiency at 609 keV, G_{BiTl} is the amount of ^{214}Bi Gaussian distribution inside ROI_{Tl}, G_{TlTl} is the amount of ^{208}Tl Gaussian distribution inside ROI_{Tl}, m_{Bi} is the fitting coefficient for the contribution from Compton scattering plus other interaction phenomena due to RD in ROI_{Bi} and m_{Tl} is the fitting coefficient for the contribution from Compton scattering plus other interaction phenomena due to RD in ROI_{Tl}.

Whenever a peak of an emission of interest is overlapped with an emission from ^{214}Bi, the calculation of the activity concentration of the isotope of interest can be easily determined without applying the method a second time, as the activity concentration of ^{214}Bi is already known. Thus, the cps corresponding to ^{214}Bi can be removed from the ROI of the isotope of interest simply using Equation (10)or(11).

For example, the 662 keV emission from ^{137}Cs overlaps with a low probability peak from ^{214}Bi at 665 keV that cannot be dismissed. Then, the activity concentration of ^{137}Cs, A_{Cs}, can be written as:

$$A_{Cs} = \frac{ROI_{Cs} - Bkgd_{Cs} - m_{Cs}\cdot A_{Bi} - c_{Cs} - A_{Bi}\cdot p_{Bi_{665}}\cdot\varepsilon_{Bi_{665}}\cdot G_{Bi_{665}Cs}}{p_{Cs}\cdot\varepsilon_{Cs}\cdot G_{CsCs}} \quad (15)$$

where ROI_{Cs} is the ROI centred around the 662 keV peak of ^{137}Cs, $Bkgd_{Cs}$ is the $LaBr_3$(Ce) intrinsic background in ROI_{Cs}, m_{Cs} is the fitting coefficient for the contribution from Compton scattering plus other interaction phenomena due to RD in ROI_{Cs}, A_{Bi} is the activity concentration

of ^{214}Bi, c_{Cs} is the contribution from Compton scattering plus other interaction phenomena due to non-RD natural emissions to ROI_{Cs}, $p_{Bi_{665}}$ is the probability of the 665 keV emission from ^{214}Bi, $\varepsilon_{Bi_{665}}$ is the detector efficiency at 665 keV, $G_{Bi_{665}Cs}$ is the amount of the Gaussian distribution from ^{214}Bi peak at 665 keV inside ROI_{Cs}, p_{Cs} is the probability of the 662 keV emission from ^{137}Cs, ε_{Cs} is the detector efficiency at 662 keV, G_{CsCs} is the amount of ^{137}Cs Gaussian distribution inside ROI_{Cs}.

3.3 $LaBr_3$(Ce) intrinsic background determination

When the method is applied at spectra obtained with $LaBr_3$(Ce) detectors, it is necessary to obtain an intrinsic background spectrum to estimate the background of each ROI. $LaBr_3$(Ce) detectors self-activity, due to ^{138}La and ^{227}Ac in the detector crystal [16], provide extra cps that must be subtracted. Therefore, the detector was placed inside a lead shielding for several hours. After the registration of the spectrum, the absence of any photopeak from natural origin was checked and an intrinsic background spectra was obtained.

3.4 Minimum Detectable Activity Concentration (MDAC)

The Minimum Detectable Activity Concentration corresponds to the activity measured from the detection limit, L_D. The detection limit is the minimum number of counts under a peak that one can be confident of detecting with a certain probability.

The MDAC can be determined as:

$$MDAC = \frac{L_D}{\varepsilon \cdot t \cdot p_\gamma} \tag{16}$$

where the detection limit L_D (with a 95% confidence limit) for a certain ROI is calculated using the expression for the standard deviation of the background [17]:

$$L_D = 2.71 + 3.29\sigma_B \tag{17}$$

where σ_B is the standard deviation of the background (laboratory plus an intrinsic background in detectors such as $LaBr_3$(Ce)) measured in counts in the considered ROI. The width of the ROI is determined by Equation (3) with $k = 1.699$ for a 95.45% peak area coverage.

3.5 Spectra analysis discrimination criterion

A discrimination criterion to identify suspicious spectra was implemented in all the monitors of the surveillance network [1], which was adapted to the spectral windows analysis method. For that, the value of the activity concentration of the isotopes associated to each ROI of every registered spectrum is obtained (x_i) and the value is checked to be in the following interval:

$$\mu - \alpha\sigma_B \le x_i \le \mu + \alpha\sigma_B \tag{18}$$

where μ is the mean value of the activity concentration of the isotope registered in a long period corresponding to the monitor site background, σ_B the standard deviation and α a confidence factor.

In this study, the confidence factor α is set at 3. Since the background follows a Gaussian distribution, values above $\mu + 3\sigma_B$ would be only the 0.135% of the measurements. Therefore, when the activity concentration of an isotope, x_i, fails the established criterion above the interval, the suspicious spectrum is analysed in detail.

4 Results

4.1 Energy and resolution calibrations

The detector was calibrated using the radioactive sources described in Section 2.1. The energy calibration of the system was performed by fitting Equation (1), giving a coefficient of determination of R^2=0.9999, whereas the energy resolution of the system was obtained using Equation (2), whose fit gave R^2=0.996.

4.2 Energy spectrum

Peak overlaps as a consequence of the limited resolution of the $LaBr_3$(Ce) can be clearly observed in the spectrum of Figure 2. To obtain this spectrum, the distances of the ^{131}I, ^{137}Cs and ^{226}Ra radioactive sources were arranged to simulate anthropogenic activities close to the MDACs (see Table 2) in a typical background environment. These distances were the same that those in scenarios 3 and 6, which are described in Section 4.3, but with all the sources placed at the same time.

The overlaps discussed in Section 3.2.4 together with the ROIs used for the different isotopes can be clearly observed in Figure 2b and Figure 2c. In this way, Figure 2b shows that the ^{214}Pb peak cannot be resolved from the ^{131}I one, and Figure 2c shows that ^{208}Tl and ^{137}Cs peaks cannot be resolved from the ^{214}Bi ones.

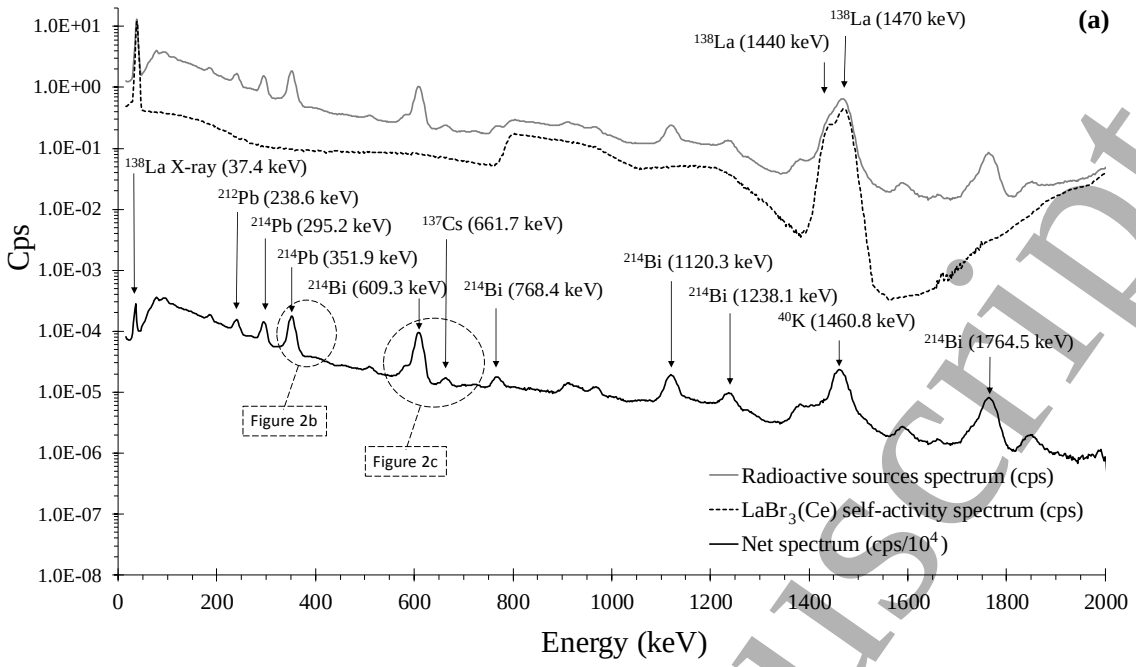

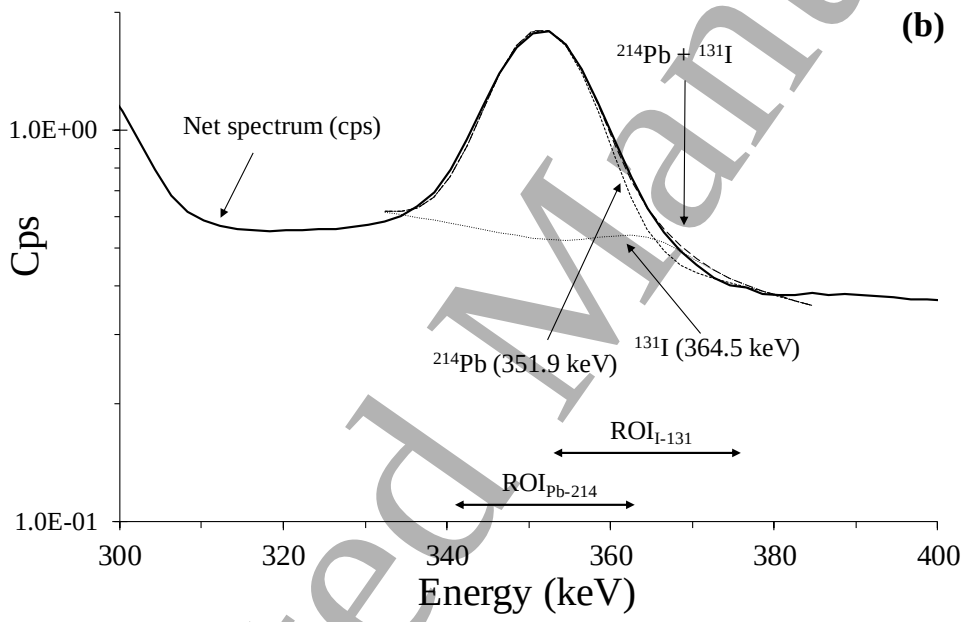

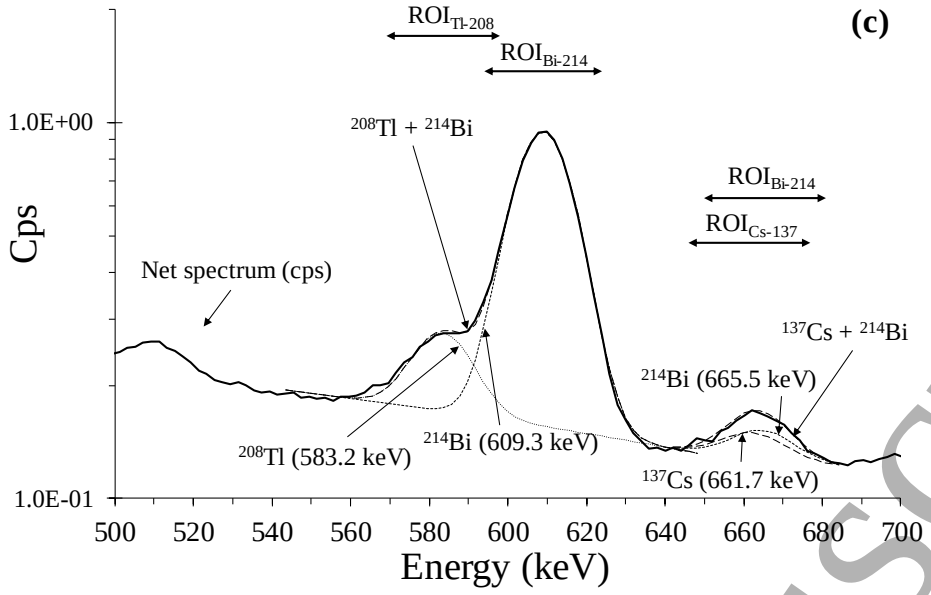

Figure 2. (a) Energy spectrum of ^{131}I, ^{137}Cs and ^{226}Ra obtained with the $LaBr_3$(Ce) detector. The distances of the radioactive sources were arranged to simulate low ^{131}I and ^{137}Cs activities (close to the MDACs) in a typical background environment. Net spectrum was obtained by removing the intrinsic background of the detector (see Section 3.3) from the obtained spectrum. For illustration purposes, net spectrum cps were divided by 10^4. (b) Zoom of the region of the ^{131}I peak (364.5 keV) showing the overlap with ^{214}Pb peak at 351.9 keV and the Gaussian fit. The widths of the considered ROIs are also represented below the peaks (c) Zoom of the region from 500 keV to 700 keV showing overlaps of ^{208}Tl and ^{137}Cs with ^{214}Bi. Gaussian fits together with the considered ROIs widths are also shown for these peaks.

4.3 Method application

Anthropogenic isotopes activity concentrations (Bq/m^3) are given for ^{131}I and ^{137}Cs, since these are typical isotopes that are susceptible of being released by a nuclear power plant in case of accident [18]. ^{214}Bi and ^{214}Pb activity concentrations are presented as a representation of the contribution from RD.

To highlight the good performance of the proposed spectral windows analysis method, it is compared with simple spectral windows analysis, where the total cps of the analysed energy window are directly converted to Bq/m^3.

4.3.1 Simple spectral windows analysis method

Figure 3 shows the activity concentration of four spectral windows corresponding to ^{137}Cs, ^{131}I, ^{214}Bi and ^{214}Pb, obtained in a series of spectra registered with a $LaBr_3$(Ce) detector in the laboratory. The isotope activities were calculated using Equation(4), subtracting only the intrinsic background of the $LaBr_3$(Ce) detector and taking into account that the width of the ROIs included the 95.45% of the peak area.

Activity concentrations were calculated from spectra registered when the detector was exposed to different radioactive sources. The radioactive sources were changed every 50 spectra, resulting in a sequence of different source scenarios. It is worth mentioning that all the different radioactive sources scenarios registered include the laboratory background. Seven different scenarios are

shown: no sources (laboratory background), ^{137}Cs, ^{137}Cs and ^{226}Ra (plus RD), ^{131}I, ^{131}I and ^{226}Ra (plus RD), ^{226}Ra (plus RD), and ^{226}Ra (plus RD) with very high activity. For illustrative purposes, the activity o concentration of the isotopes in the laboratory background was measured repeatedly along the sequence.

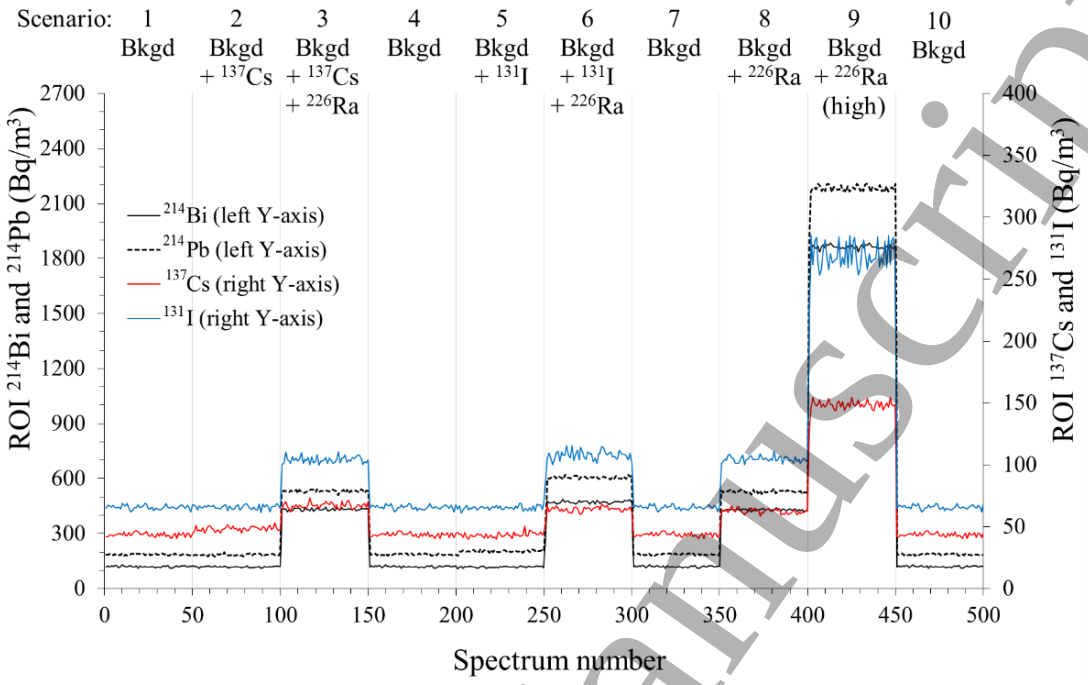

Figure 3. Activity concentrations of ^{214}Bi (black line, left Y-axis) and ^{214}Pb (dotted line, left Y-axis), ^{137}Cs (red line, right Y-axis) and ^{131}I (blue line, right Y-axis) using a simple windows analysis method. (For interpretation of the references to colour in this figure legend, the reader is referred to the web version of this article.)

4.3.2 **Proposed spectral windows analysis method**

The activity concentrations obtained for the same isotopes when applying the proposed method can be observed in Figure 4. Detailed values of the activities (mean value and standard deviation) for both methods are presented in Table 1. Additionally, values of activity concentrations obtained with the commercial software ScintiVision™ are included for comparison purposes.

It is worth to remark that the sources distances in scenarios 2, 3, 5 and 6 were arranged to simulate the most unfavourable measuring situation, corresponding to ^{131}I and ^{137}Cs activity concentrations close to the MDAC values (see Table 2) in a typical background environment.

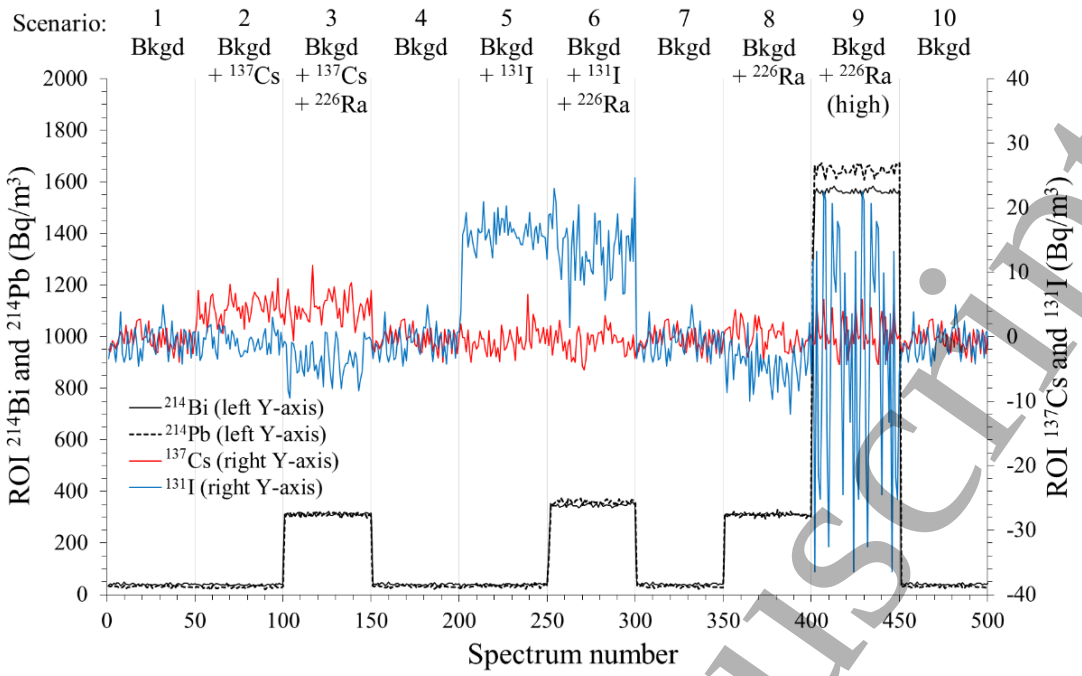

Figure 4. Activity concentrations of ^{214}Bi (black line, left Y-axis) and ^{214}Pb (dotted line, left Y-axis), ^{137}Cs (red line, right Y-axis) and ^{131}I (blue line, right Y-axis) calculated using equations of the proposed windows analysis method. (For interpretation of the references to colour in this figure legend, the reader is referred to the web version of this article.)

Scenario	External source[a]	Isotope	Activity concentration: Simple windows analysis[b] μ (Bq/m³)	Simple windows analysis σ (Bq/m³)	Proposed windows analysis method μ (Bq/m³)	Proposed windows analysis method σ (Bq/m³)	Peaks Gaussian fit μ (Bq/m³)	Δ [c] (%)
1, 4, 7 and 10	--	^{137}Cs	43.6	1.6	-0.4	1.6	0.0	n.a.
		^{131}I	65.8	1.7	-0.9	2.2	0.0	n.a.
		^{214}Bi	120	3.9	40.0	3.4	42.8	-6.9
		^{214}Pb	186	3.7	31.4	3.9	33.1	-5.2
2	^{137}Cs	^{137}Cs	48.4	1.9	4.4	1.9	4.2	5.0
		^{131}I	65.8	1.7	-0.7	1.7	0.0	n.a.
		^{214}Bi	118	3.2	38.6	2.8	40.4	-4.7
		^{214}Pb	184	4.7	29.9	4.8	31.7	-6.2
3	^{137}Cs + ^{226}Ra	^{137}Cs	67.2	2.3	4.5	2.2	4.3	3.9
		^{131}I	104	2.7	-3.6	2.8	0.0	n.a.
		^{214}Bi	432	6.1	313	5.4	315	-0.7
		^{214}Pb	531	6.7	310	6.9	313	-0.9
5	^{131}I	^{137}Cs	43.4	2.0	-0.5	2.0	0.0	n.a.
		^{131}I	65.3	1.7	15.9	2.6	12.7	19.6
		^{214}Bi	118	3.7	38.5	3.2	38.8	-0.9
		^{214}Pb	204	6.2	33.7	5.2	34.7	-3.0

6	^{131}I + ^{226}Ra	^{137}Cs	64.0	2.6	-0.8	1.9	0.0	n.a.
		^{131}I	107	4.9	16.0	4.7	10.8	21.8
		^{214}Bi	468	30.1	344	26.3	348	-1.2
		^{214}Pb	601	33.1	356	27.7	361	-1.4
8	^{226}Ra	^{137}Cs	62.6	1.9	0.1	1.9	0.0	n.a.
		^{131}I	104	2.3	-4.4	3.0	0.0	n.a.
		^{214}Bi	430	4.9	310	4.4	312	-0.4
		^{214}Pb	529	6.7	310	7.2	306	1.1
9	^{226}Ra (high activity)	^{137}Cs	148	4.1	0.4	2.7	0.0	n.a.
		^{131}I	269	11.6	-2.9	18.2	0.0	n.a.
		^{214}Bi	1857	48.0	1558	42.0	1565	-0.4
		^{214}Pb	2176	53.4	1640	46.7	1652	-0.7

[a] Intrinsic background and laboratory natural background are always included

[b] Activity concentrations obtained using Equation (4) subtracting $LaBr_3$(Ce) intrinsic background

[c] Relative percentage difference between the proposed windows analysis method and the peaks Gaussian fit results, calculated as $\Delta = 100(\mu_{Gaussian} - \mu_{proposed\_WM})/\mu_{Gaussian}$

Table 1. Comparison of the activity concentrations of ^{137}Cs, ^{131}I, ^{214}Bi and ^{214}Pb obtained with the simple and the proposed windows analysis method of the spectra registered with the different radioactive sources. Values of activity concentrations obtained with ScintiVision™ software are also presented.

4.3.3 MDAC and discrimination criterion

Table 2 shows the MDAC and the discrimination criterion values of ^{137}Cs, ^{131}I, ^{214}Bi and ^{214}Pb obtained when applying the proposed windows analysis method at 10 min background spectra (scenarios 1, 4, 7 and 10). Additionally, MDAC and discrimination criterion values plus the mean background activity concentrations are presented for each isotope.

Isotope	MDAC (Bq/m^3)	μ + MDAC (Bq/m^3)	$\Delta 3\sigma_B$ (Bq/m^3)	$\mu + 3\sigma_B$ (Bq/m^3)
^{137}Cs	5.1	4.7	4.7	4.3
^{131}I	6.9	6.1	6.6	5.7
^{214}Bi	11.0	51.1	10.3	50.4
^{214}Pb	12.3	43.7	11.6	43.0

Table 2. MDAC and discrimination criterion values obtained for ^{137}Cs, ^{131}I, ^{214}Bi and ^{214}Pb, after the application of the method.

4.3.4 Flow-chart of the complete procedure

Finally, for illustrating the complete procedure, a flow-chart showing the different steps that were performed within this study is shown in Figure 5.

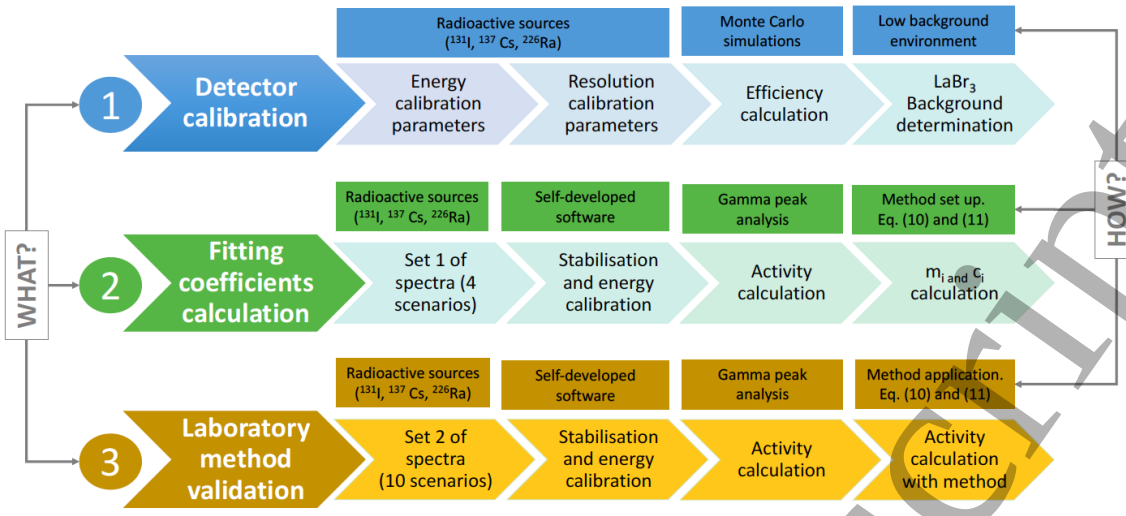

Figure 5. Flow-chart of the complete procedure, which was divided in 3 main steps, including (1) detector calibration, (2) calculation of the fitting coefficients for using the method and (3) laboratory validation of the proposed method.

5 Discussion

5.1 RD activity concentrations

The activities obtained by the windows analysis method of the ROIs that correspond to RD (^{214}Bi and ^{214}Pb), in the different sources scenarios (Table 1), are in agreement with those obtained with ScintiVision™ software, giving a maximum absolute difference lower than 7% when computing the activity concentration of ^{214}Bi of the laboratory background. It is worth noting that the relative error increases with low activities due to the difficulty of fitting smaller peaks than fitting greater ones with the commercial software.

In the simple spectral windows analysis, the increase of the activity concentration of RD is overestimated in all configurations and it is remarkable when determining the activities of spectra registered in presence of the source of ^{226}Ra. For example, the activity concentration of ^{214}Bi in scenario 9 increases 1736 Bq/m^3 from the laboratory background, whereas, after calculating the activity concentration with the proposed method, the activity concentration increases 1518 Bq/m^3. This difference is mainly due to the correction of the Compton contribution of the RD source.

Scenarios 3, 6 and 8, registered with the source of ^{226}Ra, show activities that can be obtained occasionally in field monitors of the surveillance network but are not habitual, as these activities are very high. Thus, ^{214}Bi and ^{214}Pb activities shown in scenario 9, where the ^{226}Ra source was very close to the detector, are extremely high and are never found in field measurements. However, this scenario was included to test the goodness of the methodology.

5.2 ^{137}Cs activity concentrations

With simple windows analysis method, data show presence of ^{137}Cs (43.6 Bq/m^3) in the laboratory background (scenarios 1,4, 7 and 10) whereas, after using the proposed windows method, ^{137}Cs activity concentration obtained is close to 0 for these scenarios (see Table 1). In scenarios 2 and 3, the detector is exposed to a distant source of ^{137}Cs in order to register a small increase of the

isotope activity. In Figure 3, before applying the method, the presence of ^{137}Cs is barely distinguishable from the background situation (scenarios 1 and 2) as the relative increase is low. After the application of the method, a small increment is seen in scenarios 2 and 3 (Figure 4) and an activity concentration of 4.5 Bq/m^3 is obtained.

This low activity concentration would trigger the analysis discrimination criterion for ^{137}Cs when using the proposed method, since activities over 4.3 Bq/m^3 would fulfil the criterion (see Table 2). The MDAC value obtained for ^{137}Cs for 10 min spectra is very similar to the discrimination criterion and to the 5 Bq/m^3 recommended for the minimum activity concentration of ^{137}Cs bound to aerosols detectable within 2 h in the Safety Standards of the German Nuclear Safety Standards Commission [19].

A remarkable situation is shown in scenario 3 in Figure 4, where a source of ^{226}Ra is added to the ^{137}Cs source. In simple spectral windows analysis, the presence of natural radiation is computed as an increase of ^{137}Cs activity concentration (false-positive result). However, using the proposed method, the activity concentration of ^{137}Cs remains constant and equal to scenario 2 (only ^{137}Cs source).

This effect is much more noticeable in scenario 9, where the high presence of RD increases in 104.7 Bq/m^3 the concentration of ^{137}Cs from the laboratory background when using the simple windows analysis method while it remains close to 0 when applying the proposed windows method. Therefore, the method proved to be an adequate system for establishing a ^{137}Cs early-warning alarm, as it is able to trigger the analysis criterion when low activity concentrations of ^{137}Cs are present but it does not generate false-positive results in situations with high presence of natural radiation from RD.

5.3 ^{131}I activity concentrations

Using simple spectral windows analysis method, the activities calculated show different situations resulting in misleading conclusions. On the one hand, the activity concentration of ^{131}I computed without a ^{131}I source in spectra registered in the laboratory background or in presence of the ^{226}Ra source is not null, resulting in a false-positive presence of ^{131}I (scenarios 1, 2, 3, 4, 7, 8, 9 and 10). On the other hand, the value of the activity concentration of ^{131}I in presence of a ^{131}I source (scenario 5) is lower (65.3 Bq/m^3) than the value obtained in the laboratory background spectra (65.8 Bq/m^3), causing a false-negative result (see Table 1).

However, applying the proposed windows method, the mean value of ^{131}I activity concentration is near 0 in all registered scenarios without presence of the ^{131}I source (scenarios 1, 2, 3, 4, 7, 8, 9 and 10). When the source of ^{226}Ra is present (see scenarios 3, 6 and 8 in Figure 4), the calculation of ^{131}I activity concentration with the proposed method has a high dispersion σ, which is even higher when the activity concentration of ^{226}Ra is extremely great (scenario 9).

The proposed windows method overestimates ^{131}I activity concentrations compared to the Gaussian fit performed with ScintiVision™ in all scenarios (see Table 1). However, it should be mentioned that the Gaussian fit presented some complications since ^{131}I activity was very low and its 365 keV gamma-ray overlapped with the ^{214}Pb emission at 352 keV of the laboratory background, which made it difficult to properly fit a double Gaussian.

The activity concentrations obtained for ^{131}I in presence of the source (scenarios 5 and 6) would trigger the analysis criterion, as these are larger than the 5.7 Bq/m^3 threshold (see Table 2). The MDAC obtained is of the same order as the threshold and lower than the minimum activity

concentration of ^{131}I detectable within 2 h recommended by the German Nuclear Safety Standards Commission, which is set at 20 Bq/m^3 [19]. However, in view of the great dispersion of the obtained ^{131}I activity concentrations, these results should be interpreted with caution.

In scenario 6, where the detector is exposed to ^{131}I and ^{226}Ra sources, the proposed method obtains a ^{131}I constant activity concentration, equal to that in the scenario without ^{226}Ra and only a ^{131}I source (scenario 5). The values obtained by the Gaussian fitting software are lower than those obtained by the method (Table 1). As it has been mentioned before, the reason for this is probably due to the overlapping of ^{214}Pb and to the external cps contributions to ^{131}I ROI.

5.4 General considerations

The described method was developed to be applied in spectra obtained by environmental real-time monitors using gamma-ray scintillation spectrometry with any kind of detector crystal. The presented results were particularised for a $LaBr_3$(Ce) monitor measuring directly to the environment; however, the method can be adapted to any scintillation detector, shielding geometry or monitor type after determining the adequate parameters.

In particular, the proposed method could be used with detectors having less resolution than $LaBr_3$(Ce) detectors, such as NaI(Tl) detectors. The method showed good performance despite the observed overlap in Figure 2 for both ^{131}I and ^{137}Cs, which showed that the studied peaks could not be resolved, as it would happen in a detector with lower resolution. For this reason, the method can be used for monitoring isotopes in monitors of spectrometry surveillance networks.

The method assumed that the Compton scattering contribution from natural isotopes that were not RD (e.g. ^{40}K and those from ^{232}Th decay chain, mainly ^{208}Tl, ^{228}Ac, ^{212}Bi, ^{212}Pb) plus all other types of external contributions to a spectrum were constant. In laboratory measurements, the activity concentrations from ^{40}K and ^{208}Tl were confirmed to be constant, but in field measurements the hypothesis might not still be valid, specially for ^{208}Tl. Thus, in case of finding variable external contributions to spectra when adjusting the c_i parameter for field monitors, a term $m_i' A_i$ could be added to take into account the fluctuations of non-RD isotopes.

In gamma-ray spectrometry monitors using NaI(Tl) detectors, the lower resolution of their crystal compared to $LaBr_3$(Ce) ones would contribute to a major peak overlapping. Even if the method is prepared to solve peak overlapping situations, better results are obtained for smaller overlapping of peaks inside a ROI. The overlapping could be minimised simply setting narrower ROI widths than the ones used in this study.

The analysis method presented in this paper is advantageous as it is computationally easy to implement. Moreover, the parameters used in the calculations can be obtained from a simple set of spectra measured with low dose rate radioactive sources. The possibility to fit the parameters to activity concentrations obtained with other analysis methods, for example by Gaussian fitting, guarantees that the obtained activity concentrations are in agreement with those obtained with a validated software, such as ScintiVision™.

6 Conclusions

The windows analysis method presented in this paper is a simple and useful tool for automatic monitoring of activity concentrations of natural and anthropogenic radionuclides in real-time environmental gamma-ray spectrometry with scintillation detectors, even if they are close to the MDAC values. Despite that the standard deviation of the obtained activity concentrations for ^{131}I was remarkable, the mean value was in agreement with the activity concentrations obtained with a commercial Gaussian fitting software. The method proved to be reliable when monitoring ^{137}Cs, since it did not generate false-positive neither false-negative results.

Although the presented results were obtained in laboratory conditions, the method can be adjusted to field monitors by calculating parameters related to the Compton scattering and to other external contributions arising from gamma-ray interactions with matter. In fact, further work is being performed to check the reliability of the proposed method when used in the different field monitors that are part of the environmental radioactivity surveillance network of Catalonia.

Finally, the proposed windows analysis method can be used for the establishment of early-warning alarms based on activity concentration thresholds in real-time environmental gamma-ray scintillation spectrometry without the need of using conventional peak analysis.

Acknowledgements

The authors would like to express their gratitude to the Radioactive Activities Coordination Service (SCAR) of the Government of Catalonia for the partial funding of this study within the administrative contract EMO 2015 262, Lot 2, and to the Nuclear Safety Council of Spain (CSN) for the partial funding of a R+D project published at the Spanish Official State Gazette *BOE nº 178 de 26 de julio de 2012*.

References

[1] Casanovas R, Morant J J, López M, Hernández-Girón I, Batalla E and Salvadó M 2011 Performance of data acceptance criteria over 50 months from an automatic real-time environmental radiation surveillance network *J. Environ. Radioact.* **102** 742–8

[2] Casanovas R, Morant J J and Salvado M 2014 Development and Calibration of a Real-Time Airborne Radioactivity Monitor Using Gamma-Ray Spectrometry on a Particulate Filter *Ieee Trans. Nucl. Sci.* **61** 727–31

[3] Casanovas R, Morant J J and Salvado M 2014 Development and calibration of a real-time airborne radioactivity monitor using direct gamma-ray spectrometry with two scintillation detectors *Appl. Radiat. Isot.* **89** 102–8

[4] Casanovas R, Morant J J and Salvadó M 2013 Implementation of gamma-ray spectrometry in two real-time water monitors using NaI(Tl) scintillation detectors *Appl. Radiat. Isot.* **80** 49–55

[5] Prieto E, Casanovas R and Salvadó M 2017 Calibration and performance of a real-time gamma-ray spectrometry water monitor using a LaBr 3 (Ce) detector *Radiat. Phys. Chem.*

[6] Casanovas R, Prieto E and Salvadó M 2016 Calculation of the ambient dose equivalent H*(10) from gamma-ray spectra obtained with scintillation detectors *Appl. Radiat. Isot.* **118** 154–9

[7] IAEA - International Atomic Energy Agency 1976 *Radiometric Reporting Methods and Calibration in Uranium Exploration*

[8] Korbech U and Nielsen K . 1992 A Simple Method for Early Detection of Fall-out *Radiat. Prot. Dosimetry* **40** 103–9

[9] IAEA - International Atomic Energy Agency 1991 *Airborne gamma ray spectrometer surveying*

[10] Arnold L J, Duval M, Falguères C, Bahain J-J and Demuro M 2012 Portable gamma spectrometry with cerium-doped lanthanum bromide scintillators: Suitability assessments for luminescence and electron spin resonance dating applications *Radiat. Meas.* **47** 6–18

[11] Blum P, Rabaute A, Gaudon P and Allan J F 1997 Analysis of natural gamma-ray spectra obtained from sediment cores with the shipboard scintilation detector of the Ocean Drilling Program: Example from Leg 156 *Proc. Ocean Drill. Program, Sci. Results* **156**

[12] Cresswell A J, Sanderson D C W and White D C 2006 137Cs measurement uncertainties and detection limits for airborne gamma spectrometry (AGS) data analysed using a spectral windows method *Appl. Radiat. Isot.* **64** 247–53

[13] Casanovas R, Morant J J and Salvado M 2012 Temperature peak-shift correction methods for NaI(Tl) and LaBr3(Ce) gamma-ray spectrum stabilisation *Radiat. Meas.* **47** 588–95

[14] Casanovas R, Morant J J and Salvadó M 2012 Energy and resolution calibration of NaI(Tl) and LaBr 3(Ce) scintillators and validation of an EGS5 Monte Carlo user code for efficiency calculations *Nucl. Instruments Methods Phys. Res. Sect. A Accel. Spectrometers, Detect. Assoc. Equip.* **675** 78–83

[15] Gilmore G R 2008 *Practical gamma-ray spectrometry - 2nd edition*

[16] Quarati F G A, Khodyuk I V., Van Eijk C W E, Quarati P and Dorenbos P 2012 Study of 138La radioactive decays using LaBr 3 scintillators *Nucl. Instruments Methods Phys. Res. Sect. A Accel. Spectrometers, Detect. Assoc. Equip.* **683** 46–52

[17] Currie L a. 1968 Limits for qualitative detection and quantitative determination. Application to radiochemistry *Anal. Chem.* **40** 586–93

[18] Nuclear Energy Agency 2002 Assessment of Radiological and Health Impacts 2002 Update of Chernobyl : Ten Years On *Chernobyl, Assess. Radiol. Heal. Impacts*

[19] Nuclear Safety Standards Commission (KTA) 2005 Safety Standards KTA 1502 (2013-11) Monitoring Volumetric Activity of Radioactive Substances in the Inner Atmosphere of Nuclear Power Plants